Journal of Materials Chemistry A

COMMUNICATION

View Article Online
View Journal | View Issue

Cite this: J. Mater. Chem. A, 2014, 2, 13245

Received 6th June 2014
Accepted 25th June 2014

DOI: 10.1039/c4ta02861a

www.rsc.org/MaterialsA

Highly efficient carbon dioxide capture with a porous organic polymer impregnated with polyethylenimine†

Siyoung Sung and Myunghyun Paik Suh‡*

Various amounts of a branched polyethylenimine are impregnated into a porous aromatic framework. PEI (40 wt%) ⊂ PAF-5 shows exceptionally high capacity and selectivity of CO_2 adsorption at 313 K. The material also displays fast adsorption/desorption kinetics and low energy penalty for regeneration in addition to water stability.

In order to mitigate the recent environmental crises such as global warming and ocean acidification, efficient carbon dioxide (CO_2) capture technologies from flue gas or ambient air should be developed.[1–4] Typical post-combustion flue gas from a coal-fired power plant contains N_2 (73–77%), CO_2 (15–16%), H_2O (5–7%), and other gases such as O_2 (3–4%), SO_2 (800 ppm), SO_3 (10 ppm), NO_x (500 ppm), HCl (100 ppm), CO (20 ppm), and hydrocarbons (10 ppm), with the emission temperature of 313–343 K.[1] Therefore, CO_2 capture material for flue gas should have high adsorption selectivity for CO_2 over N_2 at a low CO_2 partial pressure and outstanding water stability as well as high CO_2 uptake capacity at elevated temperatures, fast adsorption and desorption kinetics, and regenerability.[1] As CO_2 capture materials, numerous solid adsorbents such as silica[5] and carbon materials,[6] metal–organic frameworks,[7] and porous organic polymers[8–14] have been developed. In particular, some porous organic polymers have attracted great attention due to their high surface areas, low density, and excellent thermal, chemical, and water stabilities.[8–15] Especially, the low density of porous organic polymers formed by the covalent bonds of only light elements such as C, N and H may lead to high gas uptake per unit mass of the adsorbent.[11,12] In addition, the porous organic polymers display superior stability against water,[13] which is crucial for a post-combustion CO_2 capture material. Therefore, porous organic polymers must be an optimal class of CO_2 capture material provided that their selectivity for CO_2 over N_2 is also high. Zhou and co-workers significantly improved CO_2 capture ability of a porous organic polymer, PPN-6, by tethering various polyamines or ammonium sulfonate to PPN-6.[8b,14]

In this study, we impregnated various amounts of a branched PEI (M_w = *ca.* 800, water content ≤ 2%) into PAF-5 and investigated the CO_2 capture abilities of the materials (Scheme 1). PAF-5 is a porous aromatic framework with a 2D layered hexagonal structure constructed from only phenyl rings. It displays a high surface area (BET: 1503 $m^2\ g^{-1}$) as well as a large pore width (1.66 nm) and pore volume (1.57 $cm^3\ g^{-1}$).[16] We expected that flexible polymer PEI would block the large windows of PAF-5 to interfere the N_2 adsorption while CO_2 can open up the windows and enter the pores due to its high polarizability and quadrupole moment.[4] Furthermore, numerous amine functional groups of PEI would strongly interact with CO_2, which should increase the capacity and selectivity of CO_2 adsorption. Although there have been a few reports on PEI incorporation in silica materials[17–23] and metal organic frameworks (MOF),[24,25] none of them has fully met the requirements for the aforementioned post-combustion CO_2 capture material. PEI-impregnated silica materials such as FS-PEI-50[21] and A-PEI/silica[23] showed high CO_2 uptake capacities at 298 K under ambient air (1.71 and 2.26 mmol g^{-1}, respectively), but the equilibrium adsorption time (420 min and 392 min, respectively) was too long for practical applications. In the case of PEI-impregnated MOFs, PEI-MIL-101-125, a high temperature (383 K) as well as a vacuum condition should be applied for an hour to regenerate the adsorbent, resulting in a high energy penalty.[24,25] To the best of our knowledge, incorporation of PEI into porous organic polymers for CO_2 capture is unprecedented. In the present work, PEI-impregnated PAF-5 shows a remarkable increase in the CO_2 uptake capacity and selectivity for CO_2 over N_2 under 0.15 atm of CO_2 at 298, 313, and 323 K. In particular, PEI (40 wt%) ⊂ PAF-5 showed a CO_2/N_2 adsorption

Department of Chemistry, Seoul National University, Seoul, 151-742, Republic of Korea. E-mail: mpsuh@snu.ac.kr; Fax: +82-2-886-8516

† Electronic supplementary information (ESI) available: Experimental details, TGA, pore size distribution, FT-IR, additional gas sorption isotherms, gas cycling experiments, and tables for gas sorption isotherms. See DOI: 10.1039/c4ta02861a

‡ Current address: Department of Chemistry, Hanyang University, Seoul 133-791, Republic of Korea. E-mail: mpsuh@Hanyang.ac.kr; Fax: +82-2-886-8516; Tel: +82-2-2220-0922

selectivity of 2160 at 313 K, adsorbing 10.8 wt% of CO_2 under a stream of 15% (v/v) CO_2 in N_2 at 313 K within 20 min, and it was completely regenerated within 10 min at 343 K under a N_2 flow. Even after exposure to water vapor for 7 days at 313 K followed by reactivation, the material hardly loses its CO_2 adsorption capacity, demonstrating its superior water stability.

PAF-5 was prepared by a nickel(0)-catalyzed Yamamoto type Ullmann cross-coupling reaction of 1,3,5-tris-(4-bromophenyl)-benzene,[16] and then a branched PEI (M_w = *ca.* 800, water content ≤ 2%) was impregnated into PAF-5 by using the conventional wet impregnation method.[17] To impregnate PEI in PAF-5, various amounts of PEI (1.0–3.0 g) were dissolved in methanol (25 mL), and the activated PAF-5 (*ca.* 0.2 g) was added to the solutions. After the solutions were stirred and sonicated for various time periods (1–6 h), the resulting slurry was filtered and washed with methanol (10 mL × 3) to remove extra PEI adsorbed on the surface of PAF-5. The PAF-5 impregnated with various amounts of PEI was activated at 373 K under reduced pressure for 24 h (Table S1, ESI†). The amount of impregnated PEI was determined by thermogravimetric analyses (TGA) and elemental analysis data for the activated samples. In TGA, while dried PAF-5 is stable up to 873 K, PEI-impregnated PAF-5 samples show a sharp weight loss between 573 and 673 K, which is attributed to the thermal decomposition of impregnated PEI (Fig. S1†). The weight percent of PEI in PAF-5 was determined by the weight loss in this stage. In the elemental analyses, the increase in weight percent of nitrogen was observed as more PEI was impregnated into PAF-5 (Table S2†). The activated samples show a broad peak at *ca.* 3300 cm^{-1} in the IR spectrum, corresponding to the amine functional groups that form extensive hydrogen bonding (Fig. S4†).

To investigate the porosity of PAF-5 and the PEI-impregnated PAF-5, the materials were activated at 373 K under vacuum for 24 h, and N_2 adsorption/desorption isotherms were measured. The N_2 adsorption isotherm measured at 77 K indicates that pristine PAF-5 has a BET surface area of 2070 $m^2\ g^{-1}$, a pore width of 2.11 nm and a pore volume of 1.43 $cm^3\ g^{-1}$, as calculated by non-local density functional theory (NLDFT) applying the model of carbon as an adsorbent and slit pore. These values are slightly higher than previously reported values of PAF-5.[16] For PEI (x wt%) ⊂ PAF-5, N_2 uptake at 77 K decreases gradually as the weight percent of loaded PEI increases as shown in Fig. 1a and Table 1, indicating that PEI is impregnated in the pores of PAF-5 instead of the solid surface. For PEI (40 wt%) ⊂ PAF-5, the BET surface area and pore volume are reduced to less than 3% of those of PAF-5 (40.3 $m^2\ g^{-1}$ and 0.046 $cm^3\ g^{-1}$, respectively), indicating that PEI fills almost completely the channel spaces of PAF-5. It should be noted that impregnated PEI was not released even under the high vacuum condition, and this stability must be attributed to the C–H···π interactions between the ethylene groups of PEI and phenyl rings of PAF-5. N_2 adsorption and desorption isotherms of PAF-5 and its PEI-loaded samples were also measured at 298, 313, and 323 K up to 1 atm, and the data were used in the calculation of selectivity for CO_2/N_2 adsorption (Fig. S6†).

CO_2 adsorption/desorption isotherms were measured for PAF-5 and PEI-impregnated samples at 298, 313, and 323 K up to 1 atm. Pristine PAF-5 shows linearly increasing CO_2 adsorption isotherms at 298, 313, and 323 K, taking up very small amounts of CO_2 under 0.15 atm of CO_2 pressure, 1.2, 0.8, and 0.7 wt%, respectively (Fig. 1b and S7†). However, CO_2 adsorption isotherms of PEI-loaded adsorbents change to a type-I curve at all three different temperatures, resulting in a drastic increase in CO_2 uptake capacities at 0.15 atm. In particular, PEI (40 wt%) ⊂ PAF-5 adsorbs 11.7 wt%, 11.1 wt%, and 10.9 wt% of CO_2 under 0.15 atm of CO_2 pressure at 298 K, 313 K, and 323 K, respectively, which are 10, 14, and 16 times greater than those of pristine PAF-5. The drastic increase in CO_2 uptake capacity at low CO_2 pressure stems from the strong interactions between the amine groups impregnated in PAF-5 and CO_2 molecules. Isosteric heat (Q_{st}) of the CO_2 adsorption in PAF-5 and PEI-impregnated PAF-5 was calculated by using the Clausius–Clapeyron equation based on dual-site Langmuir fit parameters obtained from the adsorption isotherms at 298, 313, and 323 K (Table 1, and Fig. S8–S11†). As shown in Fig. 1c, the plot of Q_{st} values *versus* CO_2 uptake shows two distinctive regions. In particular, 30 wt% and 40 wt% PEI-loaded adsorbents display high Q_{st} values (65.8–68.7 kJ mol^{-1}) up to *ca.* 1.5 and 2.0 mmol g^{-1} of CO_2 loading, respectively, which decrease to low Q_{st} values (23.3–18.5 kJ mol^{-1}) in the higher CO_2 loading. Interestingly, the first region of high Q_{st} values covers broader ranges of CO_2 uptake capacity as more amount of PEI is impregnated in PAF-5. These clearly indicate that the first region corresponds to chemisorption of CO_2 on PEI and the second region to physisorption on the surface of PAF-5. The ratios of the adsorbed CO_2 amounts by chemi- and physisorption calculated for PEI (10 wt%) ⊂ PAF-5, PEI (30 wt%) ⊂ PAF-5, and PEI (40 wt%) ⊂ PAF-5 at 313 K, based on Fig. 1, are 0.43, 1.49, and 1.72, respectively.

The CO_2 adsorption selectivity over N_2 based on IAST (Ideal Adsorbed Solution Theory) could not be calculated, since extremely low N_2 adsorption data for the PEI-impregnated adsorbents could not be reasonably fitted. Therefore, it was calculated by using the single component adsorption isotherms by using the molar ratio of the CO_2 uptake at 0.15 atm and the

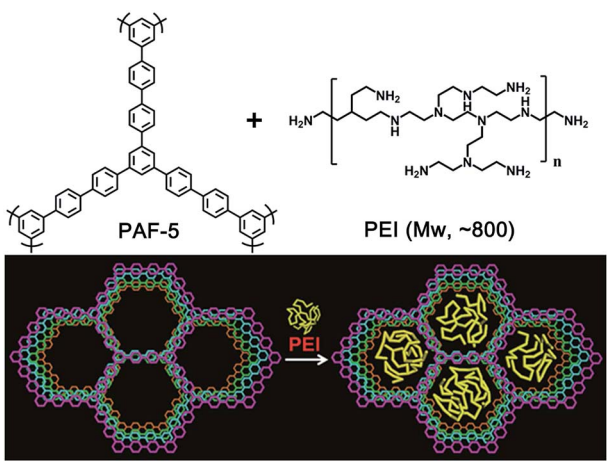

Scheme 1 Schematic description of PAF-5 impregnated with branched PEI (M_w = *ca.* 800).

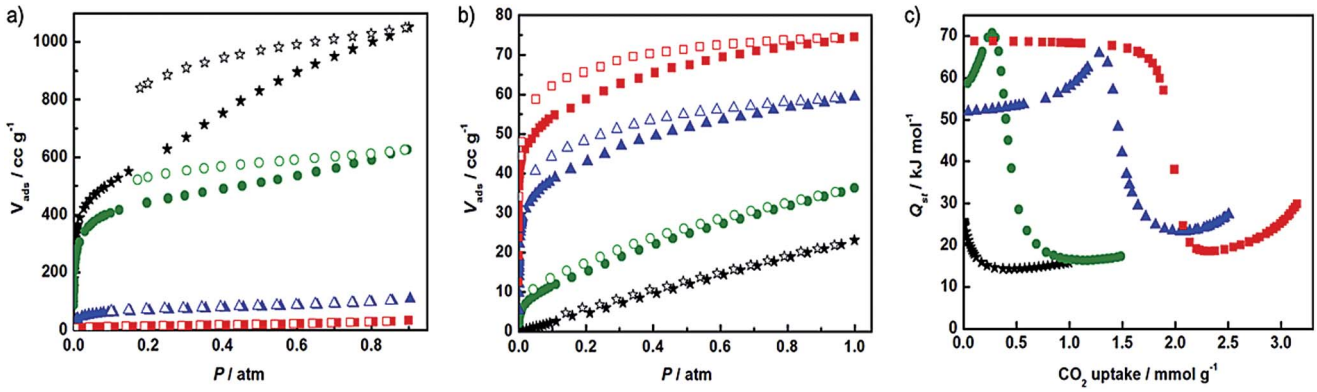

Fig. 1 Gas sorption properties of PAF-5 (★), PEI (10 wt%) ⊂ PAF-5 (●), PEI (30 wt%) ⊂ PAF-5 (▲), and PEI (40 wt%) ⊂ PAF-5 (■). (a) N_2 at 77 K. (b) CO_2 at 313 K. (c) Isosteric heat of CO_2 adsorption. Filled shapes: adsorption process; open shapes: desorption process.

Table 1 Porosity and CO_2 gas sorption properties of PAF-5 and PEI (x wt%) ⊂ PAF-5 and comparisons with the properties of other materials

			CO_2 adsorption capacity				
Compound	S_{BET}[a] (m^2 g^{-1})	V_{total}[a] (cm^3 g^{-1})	Pure CO_2[b] (wt%)	15% CO_2[c] (wt%)	Selectivity[d]	Q_{st} (kJ mol^{-1})	Ref.
PAF-5	2070 (2150)	1.43 (1.34)	1.2/0.8/0.7	0.4	9.3/9.7/15.6	26.0–14.3	This work
PEI (10 wt%) ⊂ PAF-5	1640	0.836	3.2/2.7/2.3	1.9	37.3/74.4/45.9	70.7–16.4	This work
PEI (30 wt%) ⊂ PAF-5	233	0.152	8.8/8.1/7.6	8.4	403/407/677	65.8–23.3	This work
PEI (40 wt%) ⊂ PAF-5	40.3	0.046	11.7/11.1/10.9	10.8	1200/2160/1750	68.7–18.5	This work
MC400/10PEI% 83	6.16	0.016	—	18[e]	—	—	5a
NPOF-4-NH_2	554	0.28	4.8/2.3/—	—	81/29/—[f]	30.1	10
BILP-2	708	0.49	6.4/—/—	—	113/71/—[g]	28.6	12
PPN-6-CH_2DETA	555	0.264	—/11.8[h]/10.0	—	442[i]	—	14
MCM-41-PEI-50	4.2	0.011	—/—/4.4[j]	—	—	—	17
PEI/Zr11-SBA-15	230	0.613	—	6.9[k]	—	—	20
PEI-MIL-101-125	182.9	0.095	16.9/—/17.4[l]	—	770/—/1200[f]	—	24

[a] Values are for the samples activated by the heat-evacuation method, and those in the parentheses are for PAF-5 activated by the supercritical CO_2 drying method. [b] Uptake under 0.15 atm of CO_2 in the gas adsorption isotherms measured at 298/313/323 K. [c] From the gas cycling data measured at 313 K under a stream of 15% (v/v) CO_2 in N_2. [d] Calculated by using the molar ratio of the CO_2 uptake at 0.15 atm and the N_2 uptake at 0.85 atm at 298/313/323 K. [e] Measured under a flow of 20% CO_2 in N_2 at 348 K for 120 min using a TGA. [f] Calculated by using the molar ratio of the CO_2 uptake at 0.15 atm and the N_2 uptake at 0.75 atm at 298/323 K. [g] Calculated from Henry's law constants for single-component adsorption isotherms. [h] Measured at 295 K. [i] Calculated by ideal adsorbed solution theory. [j] The weight change of the adsorbent was measured on a TGA analyzer under pure 1 atm CO_2 at 323 K. [k] Measured under a flow of 10% CO_2 in N_2 at 298 K for 12 hours using a TGA. [l] From the gas isotherm measured at 298 K and 323 K up to 0.15 atm. No desorption isotherm was reported.

N_2 uptake at 0.85 atm at 298, 313, and 323 K. For the PEI-loaded adsorbents, a sharp increase in the CO_2 uptake at low CO_2 pressure together with the large decrease in the N_2 uptake synergistically enhances the CO_2/N_2 adsorption selectivity at 298, 313, and 323 K. As shown in Table 1, PEI (40 wt%) ⊂ PAF-5 shows the highest selectivity (2160) at 313 K. To the best of our knowledge, this selectivity is the highest value reported so far for CO_2 capture materials.

To test the possibility of practical application of PEI-impregnated PAF-5 in post-combustion CO_2 capture, a gas cycling experiment was conducted on a thermogravimetric (TG) apparatus. For the adsorption process, the adsorbents were exposed to a stream of 15% (v/v) CO_2 in N_2 at 313 K, which approximately mimics flue gas. After the adsorption process, a pure N_2 stream was applied to regenerate the adsorbents at the elevated temperatures, at 313 K for PAF-5, at 323 K for PEI (10 wt%) ⊂ PAF-5, and at 343 K for PEI (30 wt%) ⊂ PAF-5 and PEI (40 wt%) ⊂ PAF-5. As shown in Fig. 2, PAF-5 and PEI (10 wt%) ⊂ PAF-5 reached an equilibrium of CO_2 adsorption quickly, within 20 min, at 313 K. They showed relatively low CO_2 uptake capacities, 0.4 wt% and 1.9 wt%, respectively, and they were regenerated in 10 min under a N_2 flow at 313 and 323 K, respectively. Contrary to these, PEI (30 wt%) ⊂ PAF-5 and PEI (40 wt%) ⊂ PAF-5 adsorbed 8.4 wt% and 10.8 wt% of CO_2, respectively, at 313 K in 20 min, and they were completely regenerated in 10 min at 343 K, significantly low desorption temperature considering their very high Q_{st} values of the CO_2 adsorption. The 10.8 wt% increase of PEI (40 wt%) ⊂ PAF-5 in the gas cycling experiment is similar to 11.1 wt% CO_2 uptake at 0.15 atm in the CO_2 single component adsorption isotherm measured at 313 K. This 10.8 wt% of CO_2 uptake under a stream of 15% CO_2 in N_2 (v/v) at 313 K is one of the highest uptake capacities ever reported. Previously reported adsorbents such as PEI/Zr14-SBA-15,[20] 65PEI/monolith,[22] PEI-MIL-101-125,[24] and

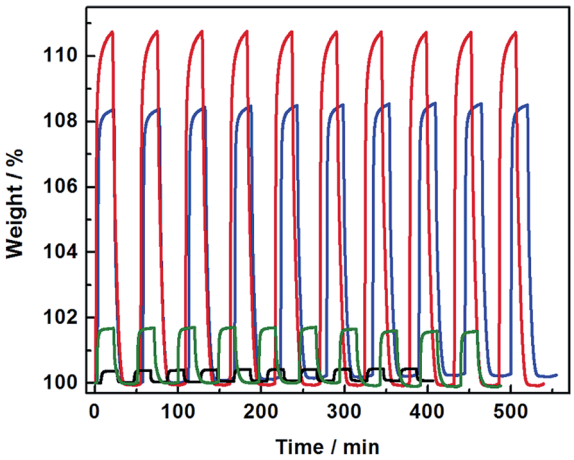

Fig. 2 Gas cycling data of PAF-5 (black), PEI (10 wt%) ⊂ PAF-5 (green), PEI (30 wt%) ⊂ PAF-5 (blue), and PEI (40 wt%) ⊂ PAF-5 (red) measured under the stream of 15% CO_2 (v/v) in N_2 at 313 K, followed by a pure N_2 stream at 323 K for PEI (10 wt%) ⊂ PAF-5, and at 343 K for PEI (30 wt%) ⊂ PAF-5 and PEI (40 wt%) ⊂ PAF-5. The adsorption and desorption time were set to 20 min in each process although the materials were completely regenerated in 10 min. The wt% in the *y* axis refers to (observed weight/initial weight) × 100.

mmen-Mg_2(dobpdc)[26] suffered from a slow adsorption (12 h)[20] or desorption process (*ca.* 100 min),[22] in addition to a high energy penalty, derived from a high regeneration temperature.[24,26] However, PEI (40 wt%) ⊂ PAF-5 in this report adsorbs a remarkably high amount of CO_2 and the material can be regenerated quickly at a slightly increased temperature (343 K). Furthermore, even after 10 cycles of adsorption/desorption, the adsorbent shows neither material decomposition nor a decrease of CO_2 uptake capacity (Fig. 2).

To exclude the possibility of cooperative N_2 adsorption[27] from a CO_2–N_2 gas mixture and validate the highly selective CO_2 adsorption in PEI (40 wt%) ⊂ PAF-5, similar gas cycling experiments were performed by using a CO_2–He mixture, since He cannot be adsorbed by any adsorbents. In the gas cycling experiment under the CO_2–He (15/85, v/v) gas mixture at 313 K, PEI (40 wt%) ⊂ PAF-5 increased its weight by 11.3 wt% within 20 min (Fig. S13†), the same as the weight increase under the CO_2–N_2 (15/85, v/v) gas mixture, and the material was completely regenerated under a N_2 stream at 353 K within 30 min. The discrepancy of 0.5 wt% under two different gas mixtures may be originated from the slight difference in the CO_2 content, and the results suggest that the material adsorbs only CO_2 from the CO_2 and N_2 gas mixture.

Since industrial flue gas contains water vapor and other acidic impurities such as SO_2, SO_3, NO_x, and HCl, the CO_2 capture material should be highly stable against water vapor and the acidic impurities. To evaluate the water stability, PEI (40 wt%) ⊂ PAF-5 was exposed to water vapor in a closed bottle for 7 days at 313 K and then activated under reduced pressure at 373 K for 48 hours. The adsorbent showed the same weight changes in the gas cycling experiment carried out under the stream of 15% CO_2 in N_2 at 313 K followed by a pure N_2 gas stream at 343 K, indicating the robustness of the adsorbent against water (Fig. S14†). Furthermore, water vapor adsorption and desorption isotherms were measured for PEI (40 wt%) ⊂ PAF-5 at 313 K (Fig. S15†). The sample adsorbed 5.0 wt% of water vapor at $P/P_0 = 0.68$, which corresponds to 0.05 atm of water vapor pressure in the post-combustion flue gas. According to the previous report by Cooper *et al.*, POPs with hydrophilic functional groups showed reduced CO_2 uptake capacity after exposure to the ambient atmosphere (~50% relative humidity conditions). In the present case also, water vapor might compete with CO_2 for adsorption on the polar PEI.[28] In addition, the acidic impurities in flue gas might react with the PEI base that is impregnated in PAF-5, and the repetitive exposure of the material to the flue gas might gradually reduce the CO_2 capture ability, even though the concentrations of acidic impurities are extremely low and PAF-5 is stable even in concentrated HCl.[12]

Working capacity of PEI (40 wt%) ⊂ PAF-5 in a temperature swing adsorption (TSA) process was also estimated by using the equation, $\Delta N = N^{ads} - N^{des}$, where N^{ads} is the amount of CO_2 adsorbed under adsorption conditions, under a flow of 15% (v/v) CO_2 in N_2, and N^{des} is the amount of CO_2 adsorbed under regeneration conditions, under a pure CO_2 stream at regeneration temperature.[29] As shown in Fig. 3, under a stream of 15% (v/v) CO_2 in N_2, PEI (40 wt%) ⊂ PAF-5 shows 11.1 wt% of CO_2 uptake at 313 K within 10 min. When the temperature was increased to 413 K at a rate of 10 K min^{-1} under a pure CO_2 stream, the sample began to lose its weight by releasing adsorbed CO_2 and was completely regenerated at 413 K. This reveals 11.1 wt% of working capacity on the TSA process between 313 K and 413 K. The CO_2 uptake capacities slightly fluctuated during the 10 cycles of TSA, showing the highest amount of CO_2 (11.7 wt%) adsorption in the 6th cycle. However, the difference of the CO_2 uptake capacities between the first and the 10th cycle is only 0.23 wt% indicating the robustness of the material (Fig. S16†).

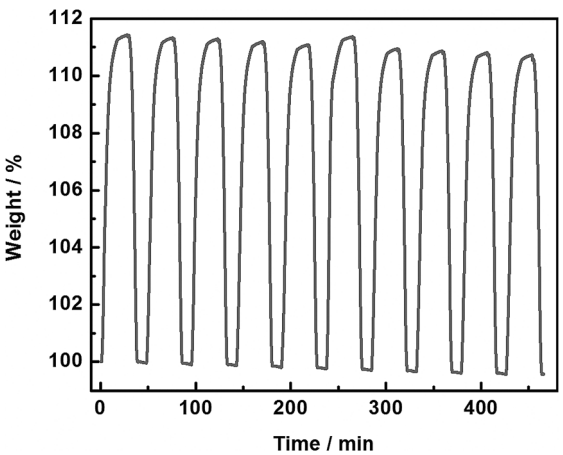

Fig. 3 Temperature swing adsorption (TSA) data of PEI (40 wt%) ⊂ PAF-5. A stream of 15% CO_2 (v/v) in N_2 was applied at 313 K for 10 min and then the temperature was increased to 413 K at a rate of 10 K min^{-1} under a stream of 1 atm CO_2. For the complete regeneration of the sample, the temperature of 413 K was maintained for 10 min. The wt% in the *y* axis refers to (observed weight/initial weight) × 100.

Conclusions

We have impregnated various amounts of a branched PEI (M_w = *ca.* 800) in PAF-5 and demonstrated that PEI (40 wt%) ⊂ PAF-5 is an effective material for CO_2 capture from the post-combustion flue gas. The material shows high CO_2 uptake capacity (11.1 wt% at 313 K under 0.15 atm of CO_2), high selectivity for CO_2 adsorption over N_2 (2160 at 313 K), fast adsorption and desorption kinetics (within 10 min.), water stability, and yet low energy penalty for regeneration of the adsorbents (413 K under 1 atm CO_2 for 11.1 wt% working capacity). For the practical application of this material in CO_2 capture from flue gas, however, we should solve several problems that are still present such as reduction of cost of the material and development of large scale up methods, which might be challenging.

Acknowledgements

This work was supported by the National Research Foundation of Korea (NRF) Grant funded by the Korean Government (MEST) (no. 2005-0093842).

Notes and references

1 K. Sumida, D. L. Rogow, J. A. Mason, T. M. McDonald, E. D. Bloch, Z. R. Herm, T.-H. Bae and J. R. Long, *Chem. Rev.*, 2012, **112**, 724–781.

2 (*a*) H. J. Park and M. P. Suh, *Chem. Sci.*, 2013, **4**, 685–690; (*b*) H. He, W. Li, M. Zhong, D. Konkolewicz, D. Wu, K. Yaccato, T. Rappold, G. Sugar, N. E. David and K. Matyjaszewski, *Energy Environ. Sci.*, 2013, **6**, 488–493.

3 (*a*) D. H. Hong and M. P. Suh, *Chem. Commun.*, 2012, **48**, 9168–9170; (*b*) T. K. Kim and M. P. Suh, *Chem. Commun.*, 2011, **47**, 4258–4260.

4 H.-S. Choi and M. P. Suh, *Angew. Chem., Int. Ed.*, 2009, **48**, 6865–6869.

5 (*a*) G. Qi, Y. Wang, L. Estevez, X. Duan, N. Anako, A.-H. A. Park, W. Li, C. W. Jones and E. P. Giannelis, *Energy Environ. Sci.*, 2011, **4**, 444–452; (*b*) X. Wang, X. Ma, V. Schwartz, J. C. Clark, S. H. Overbury, S. Zhao, X. Xuza and C. Song, *Phys. Chem. Chem. Phys.*, 2012, **14**, 1485–1492; (*c*) J. C. Hicks, J. H. Drese, D. J. Fauth, M. L. Gray, G. Qi and C. W. Jones, *J. Am. Chem. Soc.*, 2008, **130**, 2902–2903.

6 L. Wang and R. T. Yang, *J. Phys. Chem. C*, 2012, **116**, 1099–1106.

7 (*a*) W. R. Lee, S. Y. Hwang, D. W. Ryu, K. S. Lim, S. S. Han, D. Moon, J. Choi and C. S. Hong, *Energy Environ. Sci.*, 2014, **7**, 744–751; (*b*) N. Yanai, K. Kitayama, Y. Hijikata, H. Sato, R. Matsuda, Y. Kubota, M. Takata, M. Mizuno, T. Uemura1 and S. Kitagawa, *Nat. Mater.*, 2011, **10**, 1485–1793; (*c*) T. Li, J. E. Sullivan and N. L. Rosi, *J. Am. Chem. Soc.*, 2013, **135**, 9984–9987.

8 (*a*) V. Guillerm, L. J. Weselinski, M. Alkordi, M. I. H. Mohideen, Y. Belmabkhout, A. J. Cairns and M. Eddaoudi, *Chem. Commun.*, 2014, **50**, 1937–1940; (*b*) W. Lu, W. M. Verdegaal, J. Yu, P. B. Balbuena, H.-K. Jeong and H.-C. Zhou, *Energy Environ. Sci.*, 2013, **6**, 3559–3564; (*c*) S.-Y. Ding and W. Wang, *Chem. Soc. Rev.*, 2013, **42**, 548–568; (*d*) D. Wu, F. Xu, B. Sun, R. Fu, H. He and K. Matyjaszewski, *Chem. Rev.*, 2012, **112**, 3959–4015.

9 L.-H. Xie and M. P. Suh, *Chem.–Eur. J.*, 2013, **19**, 11590–11597.

10 T. Islamoglu, M. G. Rabbani and H. M. El-Kaderi, *J. Mater. Chem. A*, 2013, **1**, 10259–10266.

11 (*a*) H. A. Patel, S. H. Je, J. Park, D. P. Chen, Y. Jung, C. T. Yavuz and A. Coskun, *Nat. Commun.*, 2013, **4**, 1357; (*b*) R. Dawson, D. J. Adams and A. I. Cooper, *Chem. Sci.*, 2011, **2**, 1173–1177; (*c*) R. Dawson, E. Stockel, J. R. Holst, D. J. Adams and A. I. Cooper, *Energy Environ. Sci.*, 2011, **4**, 4239–4245.

12 M. G. Rabbani and H. M. El-Kaderi, *Chem. Mater.*, 2012, **24**, 1511–1517.

13 H. A. Patel, F. Karadas, J. Byun, J. Park, E. Deniz, A. Canlier, Y. Jung, M. Atilhan and C. T. Yavuz, *Adv. Funct. Mater.*, 2013, **23**, 2270–2276.

14 W. Lu, J. P. Sculley, D. Yuan, R. Krishna, Z. Wei and H. C. Zhou, *Angew. Chem., Int. Ed.*, 2012, **51**, 7480–7484.

15 T. Ben, H. Ren, S. Ma, D. Cao, J. Lan, X. Jing, W. Wang, J. Xu, F. Deng, J. M. Simmons, S. Qiu and G. Zhu, *Angew. Chem., Int. Ed.*, 2009, **48**, 9457–9460.

16 H. Ren, T. Ben, F. Sun, M. Guo, X. Jing, H. Ma, K. Cai, S. Qiu and G. Zhu, *J. Mater. Chem.*, 2011, **21**, 10348–10353.

17 X. Xu, C. Song, J. M. Andresen, B. G. Miller and A. W. Scaroni, *Energy Fuels*, 2002, **16**, 1463–1469.

18 S. Kim, J. Ida, V. V. Guliants and J. Y. S. Lin, *J. Phys. Chem. B*, 2005, **109**, 6287–6293.

19 X. Ma, X. Wang and C. Song, *J. Am. Chem. Soc.*, 2009, **131**, 5777–5783.

20 Y. Kuwahara, D.-Y. Kang, J. R. Copeland, N. A. Brunelli, S. A. Didas, P. Bollini, C. Sievers, T. Kamegawa, H. Yamashita and C. W. Jones, *J. Am. Chem. Soc.*, 2012, **134**, 10757–10760.

21 A. Goeppert, M. Czaun, R. B. May, G. K. S. Prakash, G. A. Olah and S. R. Narayanan, *J. Am. Chem. Soc.*, 2011, **133**, 20164–20167.

22 C. Chen, S.-T. Yang, W.-S. Ahn and R. Ryoo, *Chem. Commun.*, 2009, 3627–3629.

23 S. Choi, M. L. Gray and C. W. Jones, *ChemSusChem*, 2011, **4**, 628–635.

24 Y. Lin, Q. Yan, C. Kong and L. Chen, *Sci. Rep.*, 2013, **3**, 1859.

25 Q. Yan, Y. Lin, C. Kong and L. Chen, *Chem. Commun.*, 2013, **49**, 6873–6875.

26 T. M. McDonald, W. R. Lee, J. A. Mason, B. M. Wiers, C. S. Hong and J. R. Long, *J. Am. Chem. Soc.*, 2012, **134**, 7056–7065.

27 D. M. D'Alessandro, B. Smit and J. R. Long, *Angew. Chem., Int. Ed.*, 2010, **49**, 6058–6082.

28 R. Dawson, L. A. Stevens, T. C. Drage, C. E. Snape, M. W. Smith, D. J. Adams and A. I. Cooper, *J. Am. Chem. Soc.*, 2012, **134**, 10741–10744.

29 Y. S. Bae and R. Q. Snurr, *Angew. Chem., Int. Ed.*, 2011, **50**, 11586–11596.